ELSEVIER

HIGHLIGHTED PAPER

RESEARCH: Original Research

Molding, patterning and driving liquids with light

Feng Lin [1,2,3], Aamir Nasir Quraishy [4,5], Runjia Li [6], Guang Yang [7], Mohammadjavad Mohebinia [7], Tian Tong [3], Yi Qiu [3,8], Talari Vishal [6], Junyi Zhao [3,9], Wei Zhang [10], Hong Zhong [1,2], Hang Zhang [1,2], Chaofu Zhou [1,2], Xin Tong [1,2], Peng Yu [1], Jonathan Hu [10], Suchuan Dong [11], Dong Liu [6], Zhiming Wang [1,2,*], John R. Schaibley [4,*], Jiming Bao [3,7,12,*]

[1] Institute of Fundamental and Frontier Sciences, University of Electronic Science and Technology of China, Chengdu, Sichuan 610054, China
[2] Yangtze Delta Region Institute (Huzhou), University of Electronic Science and Technology of China, Huzhou 313001, China
[3] Department of Electrical and Computer Engineering, University of Houston, Houston, TX 77204, USA
[4] Department of Physics, University of Arizona, Tucson, AZ 85721, USA
[5] James C. Wyant College of Optical Sciences, University of Arizona, Tucson, AZ 85721, USA
[6] Department of Mechanical Engineering, University of Houston, Houston, TX 77204, USA
[7] Materials Science and Engineering, University of Houston, Houston, TX 77204, USA
[8] School of Science, Southwest Petroleum University, Chengdu, Sichuan 610500, China
[9] Department of Electrical and Systems Engineering, Washington University in St. Louis, St. Louis, MI 63130, USA
[10] Department of Electrical and Computer Engineering, Baylor University, Waco, TX 76798, USA
[11] Department of Mathematics, Purdue University, West Lafayette, IN 47907, USA
[12] Department of Physics and Texas Center for Superconductivity, University of Houston, Houston, TX 77204, USA

When a laser beam induces surface tension gradient at the free surface of a liquid, a weak surface depression is expected and has been observed. Here we report giant depression and rupture in "optothermocapillary fluids" under the illumination of laser and sunlight. Computational fluid dynamics models were developed to understand the surface deformation and provided desirable physical parameters of the fluid for maximum deformation. New optothermocapillary fluids were created by mixing transparent lamp oil with different candle dyes. They can be cut open by sunlight and be patterned to different shapes and sizes using an ordinary laser show projector or a common laser pointer. Laser driving and elevation of optothermocapillary fluids, in addition to the manipulation of different droplets on their surface, were demonstrated as an efficient controlling method and platform for optofluidic operations. The fundamental understanding of light-induced giant depression and creation of new optothermocapillary fluids encourage the fundamental research and applications of optofluidics.

Keywords: Optothermocapillary fluids; Marangoni convection; Surface deformation; Optical molding and patterning; Laser remote manipulation

* Corresponding authors.
E-mail addresses: Wang, Z. (zhmwang@uestc.edu.cn), Schaibley, J.R. (johnschaibley@email.arizona.edu), Bao, J. (jbao@uh.edu).

 https://doi.org/10.1016/j.mattod.2021.10.022

Introduction

The deep-rooted perception of mirror-like reflection from quiescent water is because free surface of a liquid pool is perfectly flat and almost nobody has experienced the deformation of a surface by light in everyday life. Scientifically, it is possible to deform a liquid surface by making use of its interaction with light. Ashkin and Dziedzic were the first to experimentally use radiation pressure of nanosecond pulse laser with kW peak power to deform water surface [1]. Later, Komissarova et al. irradiated water with a MW peak power laser pulse and observed a transient submicrometer surface depression from holographic interference fringes [2]. Radiation pressure is certainly too weak to produce significant surface deformation because it must overcome the combined effect of gravity and surface tension that stabilizes the free surface. Costa and Calatroni were the first to use a continuous-wave (CW) He-Ne laser to thermally induce surface tension gradient and produce surface depression in a thin film of light-absorbing heavy oil [3–5]. The underlying thermocapillary forces were later used by Helmers and Witte to create a 2.5-μm surface depression in ink water with a 4-W CW laser [6]. In both cases, surface depression, was produced owing to the negative temperature coefficient of surface tension of the liquids. The amplitude of surface depression was still too small to be observed with naked eyes and ordinary photography [3–7].

On the other hand, surface tension-induced interfacial deformation and convection flow is instrumental to a myriad of applications including lithography [8–10], Marangoni convection and mass transport [7,11], alloy welding [12,13], surface capillary wave [14,15], 3D printing [16,17], microfluidics [18–21], dynamic grating [22] and adaptive optics [23–25] and crystal growth [26]. However, theoretical understanding of surface-tension-induced fluid dynamics has been slow progress. It took more than 50 years to identify the role of surface tension in the formation of flow patterns in Bénard cells [27,28]. For a thin liquid film with thickness h, the depth of surface depression Δh driven by a local surface tension difference $\Delta\sigma$ follows as $2h\Delta h + (\Delta h)^2 = 3\Delta\sigma/\rho g$ [29]. This simple expression is obtained by assuming temperature inhomogeneity and thermocapillary flow only exist in the lateral direction. For small Δh, we have $\Delta h = 3\Delta\sigma/(2\rho g h)$, indicating that the deformation approaches zero for deep fluid. Rigorous treatments of thermocapillary fluid motion induced by free surface or substrate heating were later developed [30–38]. However, possibly due to the lack of experimental realizations, these theoretical treatments were limited to thin liquid layers and no insight was provided as to what physical properties of a liquid are responsible for the surface deformation, as well as how to achieve significant surface depression. Consequently, the generation of giant surface deformation by light is of great interest to both scientific curiosity and technological applications but, yet, remains a grand challenge [23,39,40].

In this work we report a full understanding of the fundamental mechanisms governing light-induced surface deformation and demonstrate, for the first time, the rational design and creation of novel optothermocapillary fluids that exhibit giant surface deformation and can be molded by laser and sunlight. We then developed full-scale computational fluid dynamics (CFD) models that are capable of not only explaining the dependence of surface deformation on liquid thickness but also identifying optimal factors that can be used to design and formulate new optothermocapillary fluids. To demonstrate our understanding and to inspire public interest in science, we simply created a series of cost-effective optothermocapillary fluids by mixing transparent lamp oil with different candle dyes. These colorful fluids can be cut open semi-permanently by sunlight, and they can be patterned or directly inscribed with all kinds of shapes and sizes using an ordinary laser show projector and pointer. Besides the patterning and molding, the giant surface tension gradient and deformation were also demonstrated as a driving strategy for the horizontal transport and vertical elevation of optothermocapillary fluids. Furthermore, we used this phenomenon to demonstrate driving of a water droplet and a chemical reaction of solution droplets on the fluid's surface to further promote its optofluidic applications.

Results and discussion

We started surface depression experiments with a ferrofluid because of its strong optical absorbance. Ferrofluid is a so-called "magic" liquid and is best known for its astonishing surface spikes generated by a magnetic field [41]. Surprisingly, its surface can also be deformed by laser beams. Fig. 1a–c show the process of strong deformation and even breakup of 1 mm ferrofluid layer under illumination of 1 W 532 nm CW laser. To better understand the deformation mechanism, we recorded the surface deformation under lasers at three different wavelengths but with the same power. Fig. 1d-l indicate that the surface deforms more rapidly with shorter laser wavelength. Unless otherwise specified, the results discussed hereafter were obtained for a laser wavelength of 532 nm. The laser was either filtered out or blocked to obtain better images of surface deformation.

The observation of a complete exposure of the substrate to the incident laser beam through the rupture of ferrofluid suggests laser-induced thermocapillarity as the driving force because the radiation pressure will disappear once the laser beam loses a direct contact with the liquid. This conclusion is confirmed by the observation of typical Marangoni convection (Supplementary Video S1) that the fluid in the top surface experienced a rapid outward flow from the laser focus point while an inward flow toward the beam center at the bottom of the liquid layer [27,28]. The dependence of the formation dynamics on the laser wavelength can be explained from this laser-induced thermocapillary convection and the absorption spectrum. As shown in Fig. 2a, shorter wavelength gives rise to stronger optical absorption; in turn, results in greater local heating, hence greater surface tension gradient. Fig. 2b shows that the depression depth increases almost linearly with increasing of laser power, in agreement with the previous study with water [6]. Here a home-built scanning probe station is used to measure the surface deformation (Fig. S2). However, Fig. 2c reveals a dramatic impact of the liquid thickness on the depression depth: there seems to exist two critical thicknesses, a lower one (1 mm for 200 mW laser) below which the depression increases so drastically that the liq-

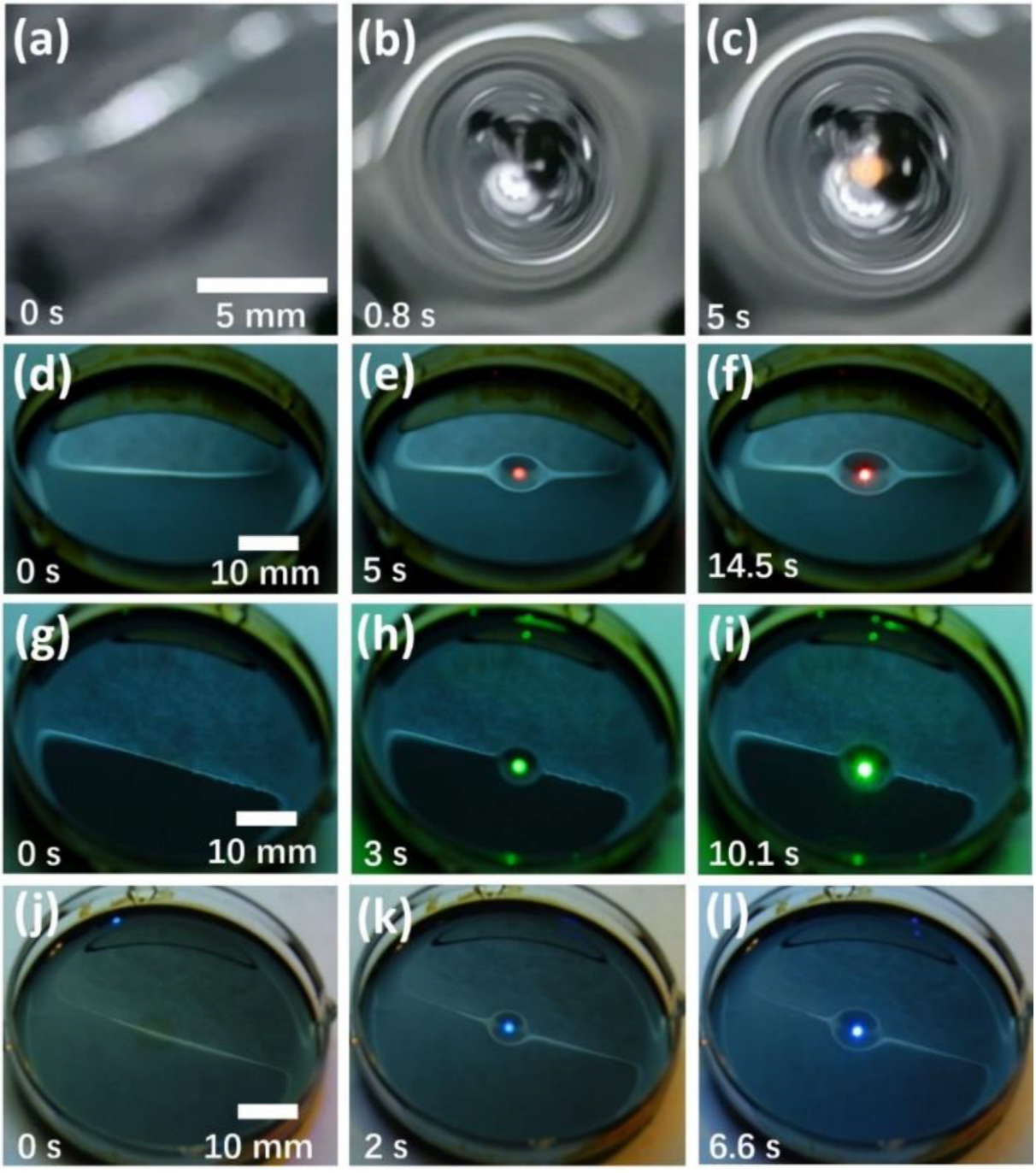

FIGURE 1

Time evolution of depression in ferrofluid by lasers with different wavelengths. (a–c) Ferrofluid depression evolves from initial flat surface to the breakup of liquid, and the breakup extends to stationary state, leaving the solid substrate partially exposed. The ferrofluid with thickness of 1 mm was irradiated by 1 W 532 nm laser. The laser is blocked by 532 nm notch filter in front of camera. (d–l) Snapshots of the development of a dip from initial flat free surface to the breakup of the liquid under 14.5 mW continuous-wave lasers with wavelengths of (d–f) 633 nm, (g–i) 532 nm and (j–l) 473 nm. The thickness of ferrofluid is 500 μm.

uid eventually ruptures, and an upper one (2.8 mm for 200 mW laser) beyond which the depression becomes less appreciable and approaches zero. In the intermediate thickness, the depression roughly follows Landau's formula [32]. The breakup of free surface has been frequently observed in very thin liquid layer and modeled analytically as a nonlinear behavior of the liquid film [32,36]. With the rising of liquid thickness, the rupture threshold laser power increases exponentially as shown in Fig. 2d.

Although ferrofluid is a nanofluid that is made of superparamagnetic nanoparticles suspended in hydrocarbon oil, it does not exhibit any magnetism in the absence of an external magnetic field, and can still be well characterized as a homogeneous liquid [25,41]. Thus, we used the physical properties of the ferrofluid and the computational fluid dynamics (CFD) model to understand the giant surface deformation and its dependence on the liquid thickness. We chose CFD simulation because it allows us

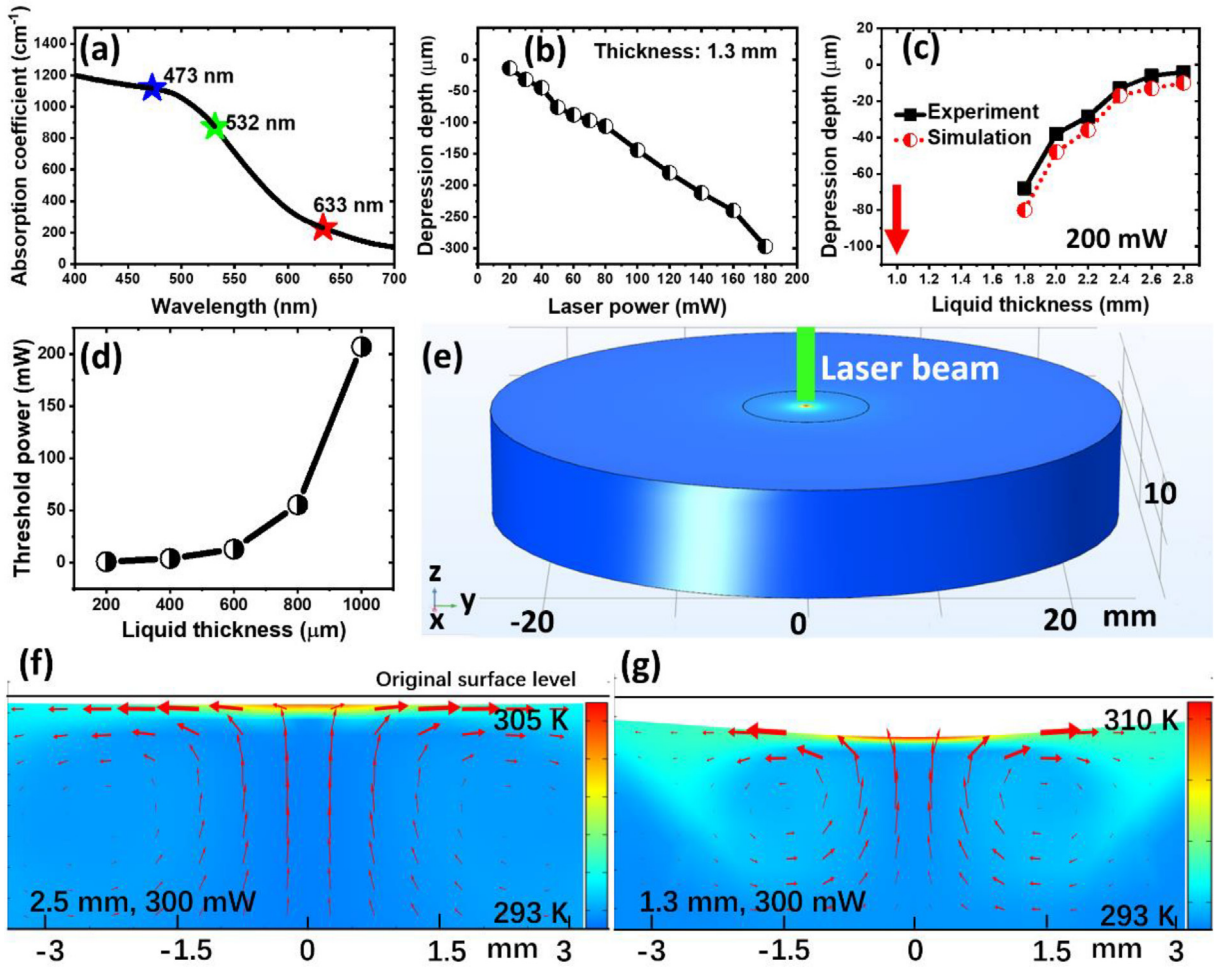

FIGURE 2

Surface depression in ferrofluid. (a) Optical absorption spectrum. (b) Depression as a function of laser power for 1.3-mm thick ferrofluid. (c) The effect of thickness on the depression depth with 200 mW laser powers. The red arrows indicate the rupture of the liquid. (d) The rupture threshold power of ferrofluid with different thickness. (e) COMSOL simulation model. (f–g) Flow and temperature fields in (f) 2.5-mm thick and (g) 1.3-mm thick ferrofluid.

to handle liquids with nearly arbitrary thickness and geometry without having to make simplifying approximations as mandated by analytical approaches. Fig. 2e shows the COMSOL simulation model, which assumes a cylindrical symmetry under a vertically incident Gaussian laser beam. Here we modeled the laser to be coupled with ferrofluid through its optical absorption. Simulation results in Fig. 2f and g clearly confirm a much larger depression in a shallower ferrofluid. The difference in depression depth can be understood from the thermocapillary-driven flow and temperature distributions. The depression is due to the outflow of liquid from the laser-illuminated region where higher temperature results in lower surface tension. Hence, the depression depth is determined by the competition between the outflow and the recirculation flow that comes from the surrounding colder region to replenish the space below the laser spot. With a shallow fluid, the flow resistance imposed by the bottom of the container (*i.e.*, the viscous shear force) is more significant and will hinder the recirculating flow, thereby leading to a larger depression.

The success of the CFD simulation encouraged us to use it as a parametric tool to study what makes ferrofluid unique and what parameters determine the deformation. Toward that end, we obtained the optical, thermal and hydrodynamic properties of ferrofluid and then systematically investigated the effect of these parameters on the deformation. The results in Fig. 3a–c show that the surface depression increases in proportion to the temperature coefficient of surface tension, whereas it decreases with larger thermal conductivity and heat capacity. The negative effects of the latter two parameters are understandable since they tend to reduce surface temperature gradient. Fig. 3d shows that there is an optimal absorption coefficient, because a very thin layer of heated surface by a highly absorbed laser cannot create an efficient volume mass transfer of fluid from the laser-irradiated spot. Fig. 3e shows that a large viscosity will enhance deformation due to a slower recirculating flow. Unlike other parameters, viscosity can vary significantly. From the foregoing analysis, it appears that the surface deformation effect is not unique to ferrofluid. We hypothesized that appreciable surface deformation should be possible in a fluid with the proper combination of physical properties. Fig. 3f shows the calculated depression of three other fluids in comparison to ferrofluid. Kerosene is comparable with ferrofluid, and pump oil has a much better performance than fer-

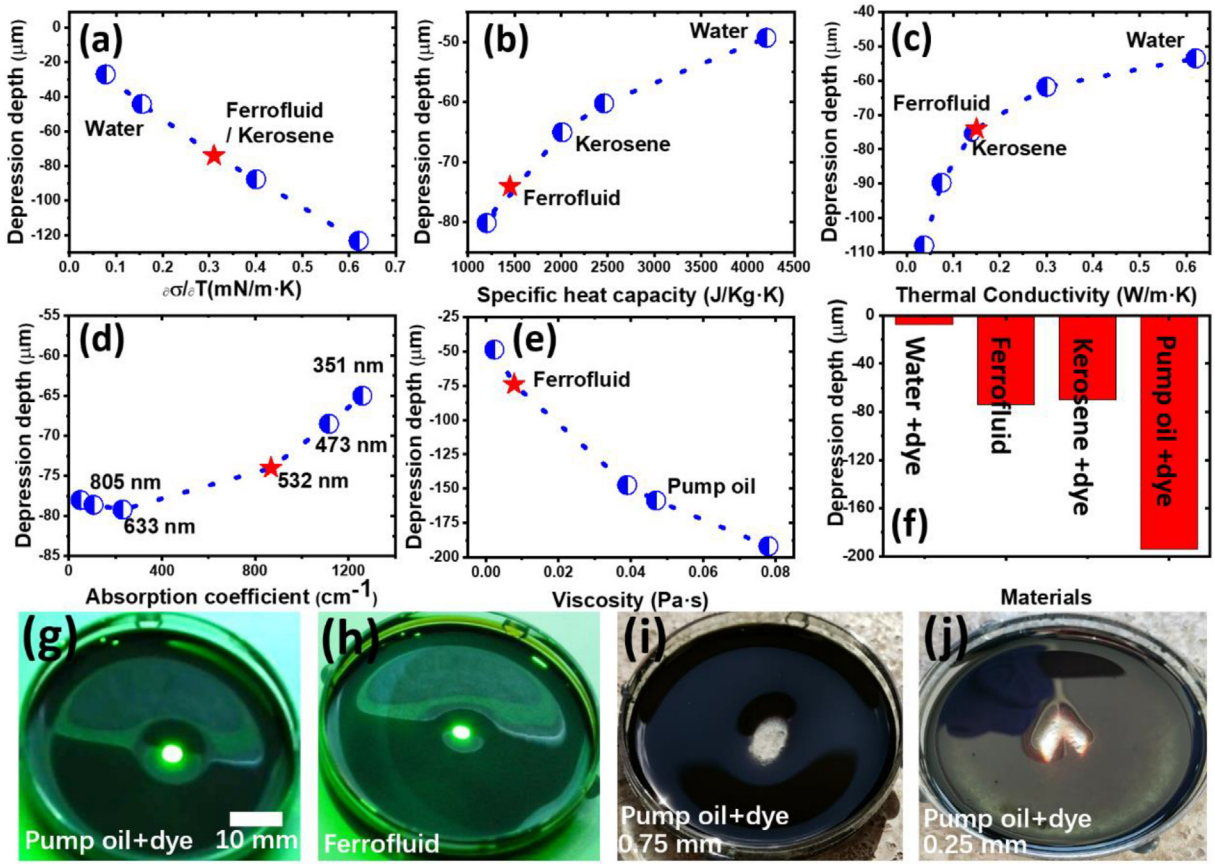

FIGURE 3

Dependence of the depression on major physical parameters of a fluid and creation of new optothermocapillary fluids. (a–e) Dependence of depression depth on (a) temperature coefficient of surface tension, (b) thermal conductivity, (c) specific heat capacity, (d) absorption coefficient and (e) viscosity. (f) Calculated depression depth for 4 fluids. Water is assumed to have the same absorption coefficient as ferrofluid, while the absorption coefficient of kerosene and pump oil is 50 cm^{-1} based on actual measurement. The thickness of fluids is 2 mm, laser power is 300 mW for all Fig. 3a–f. (g–h) Depression of 1 mm thick dyed pump oil and ferrofluid under the same laser power. (i, j) Breakup and patterning of dyed pump oil with (i) slightly focused sunlight and (j) through an aluminum foil carved with a Λ (arrow) symbol.

rofluid due to its six times higher viscosity, whereas ink water is not an excellent optothermocapillary fluid, as expected. To qualitatively verify these predictions, we used dark candle dye to increase the optical absorbance of lab pump oil. Fig. 3g-h show that a much larger depression was observed in the pump oil under the same laser. Such a high optical deformability allows us to use natural light instead of laser. Fig. 3i-j demonstrate the breakup and patterning of pump oil using slightly focused sunlight.

We want to emphasize that this is the first explicit and thorough study of the dependence of surface deformation of optothermocapillary fluid on its thermophysical properties. These simulation results have not only helped us to understand the origin of giant depressions in ferrofluid, but also provided us a recipe to develop new fluids. The large depression of dyed pump oil makes it possible to create different optothermocapillary fluids. As kerosene is the solvent of this ferrofluid, we combined household lamp oil with colorful dyes to fabricate new fluids, and we compared their optothermocapillary properties with that of the ferrofluid. With illumination of shape-controlled light and laser, the ferrofluid and the colored optothermocapillary fluids can be patterned and molded. Fig. 4a–e and Supplementary Video S2 exhibit the direct inscriptions of letters or symbol on the ferrofluid thin films with laser pointers. This simple and low-power inscription on fluid provides an economic educational model of the optothermocapillary effect and promotes its application in mask-free or reusable mask lithography. Fig. 4f–k show pictures of kerosene colored with candle dye, illuminated by slightly-focused sunlight. Fig. 4l–q show their corresponding pictures after the lens is removed. The clear image of the underlying pavement from previous bright spot in otherwise opaque oil indicates the breakup of lamp oil under the sun light. This property also enabled us to create arbitrary patterns on colored lamp oils. To do that, we used a commercial laser show projector to create a variety of patterns. These patterns can be seen in Fig. 4r–u in the orange and dark lamp oils. A video in ferrofluid is also included as Supplementary Video S3. Note that lamp oil has a viscosity as low as that of water, its opening and breakup by light is a result of strong thermocapillary force.

The light-induced deformation of liquid is the mass transfer process of Marangoni effect, thus allowing for the manipulation

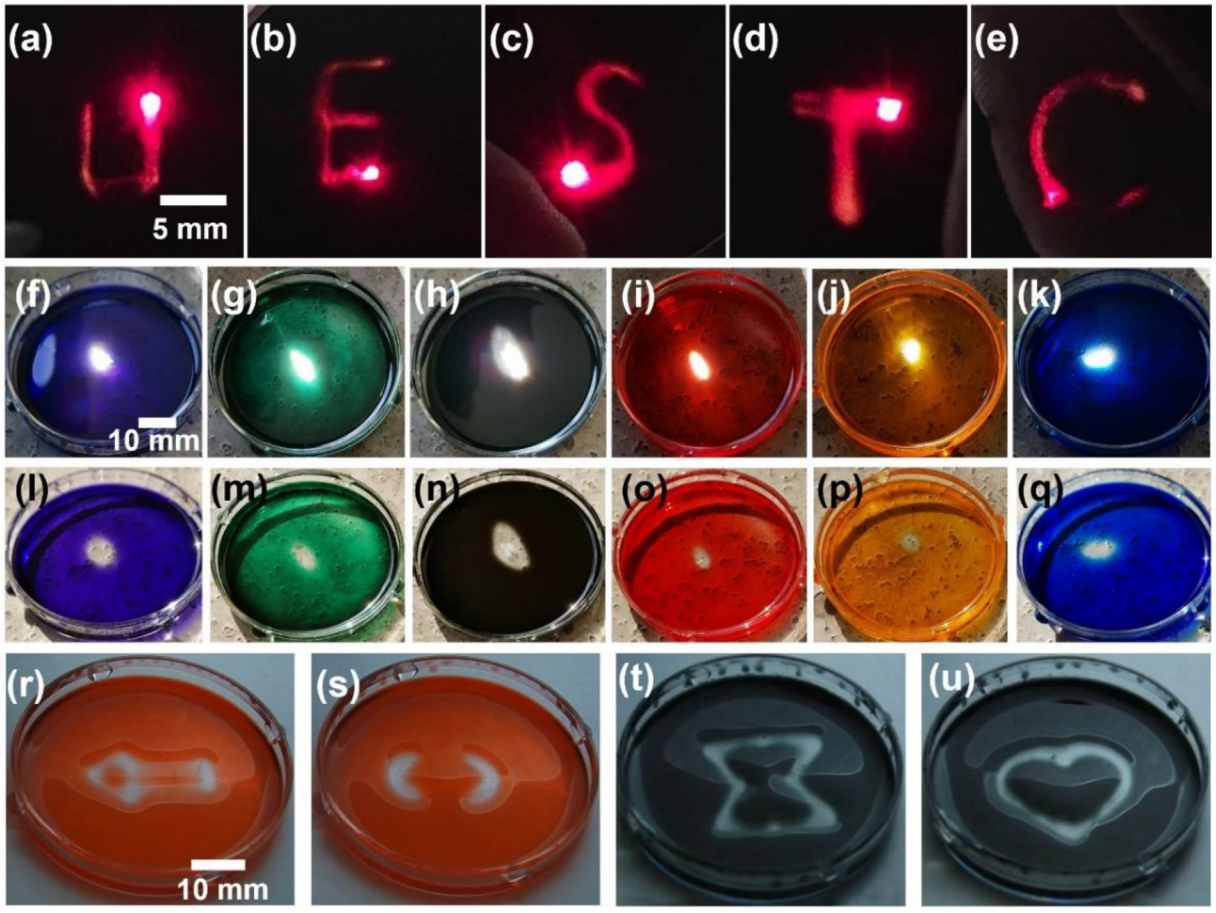

FIGURE 4

Molding of ferrofluid and colored optothermocapillary fluids made of kerosene and candle dyes. (a–e) Letters written on ferrofluid film with a common commercial laser pointer. The thickness of ferrofluid is 20 μm. The 633-nm laser is focused by lens with 15 cm focal length. (f–k) Photos of 6 colored optothermocapillary fluids under slightly focused sunlight. (i–q) Corresponding photos of (f–k) right after the lens is removed. (r–u) Molding and patterning of a (r–s) red and (t–u) dark optothermocapillary fluids by an ordinary green (532 nm, 150 mW) laser show projector. The optothermocapillary fluids in (f)–(u) are made of kerosene and candle dye with thickness of 500 μm.

of a large amount of fluid by moving the laser beam. Fig. 5a–c show the driving of ferrofluid mound horizontally with ring-shaped laser where the mound and surrounding ring follows the laser movement (Supplementary Video S4). Fig. 5d–g demonstrate the elevation of a large column of red lamp oil inside a glass tube by vertically moving the laser spot below the lamp oil (Supplementary Video S5). This elevation was achieved by inducing a large surface tension gradient between the top and bottom surfaces with a laser beam. Vertical translation of a fluid through laser has not been achieved with conventional fluids without a complex tube design, so our results suggest for a potential actuator for other liquids [19]. Besides the direct transport of an optothermocapillary fluid with strong Marangoni effect, it is also possible to manipulate other liquid droplets on the free surface of an optothermocapillary fluid. Fig. 5h-j show the laser-controlled driving of a water droplet on a ferrofluid surface, and Fig. 5k–m exhibit an example of laser-controlled chemical reaction of Na_2S and $Zn(CH_3COO)_2$ solution droplets on a ferrofluid surface. Therefore, an optothermocapillary fluid surface can be applied as a platform to manipulate the movement of various liquids.

Conclusion

To summarize, we have demonstrated macroscopic depression of ferrofluid through optothermocapillary methods and investigated the effects of material's physical parameters on the depression depth to achieve significant surface depression. We then showed the creation of new optothermocapillary liquids through the engineering of its physical properties and the light-induced patterning and molding of the fluids. We also demonstrated the direct driving and manipulation of optothermocapillary fluids and various liquid droplets on a ferrofluid surface. Our development of these fluids and the optical control of various liquids provide a new platform to explore novel optofluidic phenomena, as well as an efficient method to actuate and manipulate fluid. The giant surface deformation and its non-contact optical manipulation will enable new applications in adaptive optics [23–25], mass transport and microfluidics [7,18,42–44], 3D manufacturing and molding [8,45,46] as well as numerous applications already found by thermocapillary fluids [21,39,40]. Thus, our development of optothermocapillary fluids and its novel optofluidic phenomena has opened up a new field of interdisciplinary research and a wide range of technological applications.

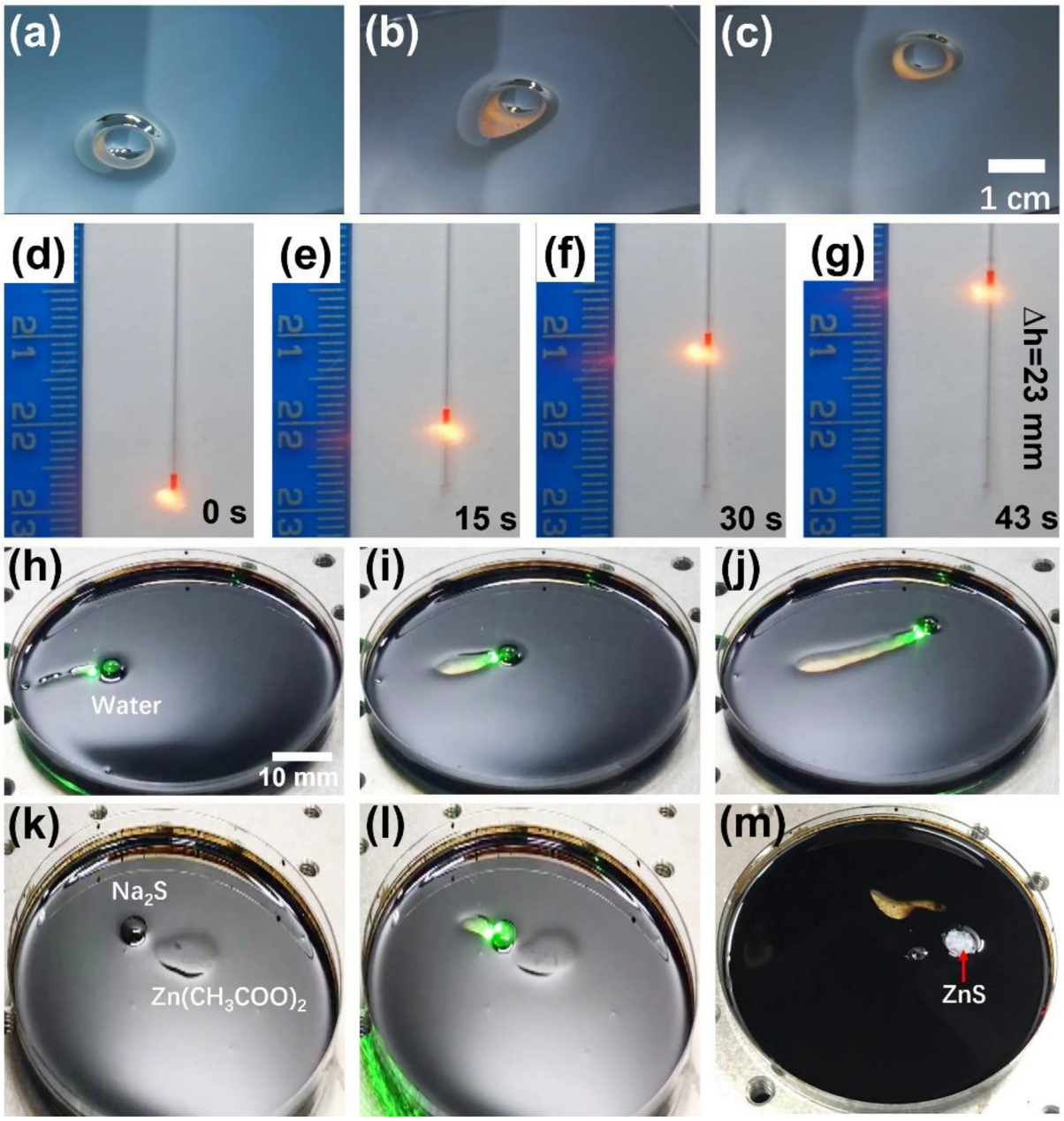

FIGURE 5

Laser manipulation of various droplets on ferrofluid surface and driving of colored optothermocapillary fluid made of kerosene and candle dyes. (a–c) Carrying of ferrofluid droplet by a ring-shape laser generated through an axicon. The 532 nm laser power is 1.5 W, and the thickness of the ferrofluid is 500 μm. (d–g) Snapshots of a column of red optothermocapillary fluid vertically elevated by a 1.5 W 532 nm laser beam. The laser in (a–g) is blocked by 532 nm notch filter in front of camera. (h–j) Carrying of a water droplet on a ferrofluid surface by a laser. (k–m) Laser-controlled reaction of Na_2S and Zn $(CH_3COO)_2$ solution droplets. The laser power is 1 W, and the ferrofluid thickness is 500 μm.

Material and methods

Materials

The ferrofluid (EFH1) was purchased from Ferrotec Corporation. The kerosene (CAS No. 64742-47-8) used in this work is Crown Kerosene 1-k and the pump oil is VWR Vacuum pump oil 19 (Cat no. 54996-061). The dye used in mixing with kerosene and vacuum pump oil is the candle making liquid colorants (KINGFINGER DIY Soy Candle Dye). The colored kerosene was prepared by mixing 2 ml kerosene with 650 μl candle dye.

Experiment setup and measurement

The surface tension temperature coefficient of the ferrofluid was measured with an optical tensiometer (KSV Attension Theta) as 0.31 mN/m·K. The dynamic viscosity as function of temperature was measured with a rheometer (HAAKE RS600) as shown in Fig. S1. The sunlight was shaped by aluminum foil carved with hole or other symbols to generate depression of dyed kerosene or pump oil. The laser show projector is LaserDock LD 1000 system. The laser ring was generated by axicon (Thorlabs AX2520-

A). The glass tube in vertical levitation of dyed kerosene has diameter of 1 mm. The surface deformation under laser irradiation was measured with a high-resolution scanning probe stage (shown in Fig. S2).

Simulation

The simulation was performed with COMSOL 5.5, and the step-by-step simulation model instructions are provided in the Supplementary data.

CRediT authorship contribution statement

Feng Lin: Conceptualization, Methodology, Formal analysis, Investigation, Writing – original draft, Writing – review & editing, Visualization, Funding acquisition. **Aamir Nasir Quraishy:** Conceptualization. **Runjia Li:** Methodology, Formal analysis. **Guang Yang:** Investigation. **Mohammadjavad Mohebinia:** Methodology, Formal analysis. **Tian Tong:** Investigation. **Yi Qiu:** Investigation. **Talari Vishal:** Investigation. **Junyi Zhao:** Investigation. **Wei Zhang:** Methodology, Formal analysis. **Hong Zhong:** Investigation. **Hang Zhang:** Investigation. **Chaofu Zhou:** Investigation. **Xin Tong:** Investigation, Resources. **Peng Yu:** Investigation, Resources. **Jonathan Hu:** Methodology, Formal analysis. **Suchuan Dong:** Methodology, Formal analysis. **Dong Liu:** Methodology, Formal analysis, Resources, Writing – review & editing. **Zhiming Wang:** Supervision, Project administration, Resources, Funding acquisition, Conceptualization, Methodology, Formal analysis. **John R. Schaibley:** Conceptualization, Methodology, Formal analysis, Project administration. **Jiming Bao:** Conceptualization, Methodology, Formal analysis, Resources, Writing – original draft, Writing – review & editing, Supervision, Project administration, Funding acquisition.

Declaration of Competing Interest

The authors declare that they have no known competing financial interests or personal relationships that could have appeared to influence the work reported in this paper.

Acknowledgements

F. L. and Z. M. W. acknowledge support from NSFC (No. 62075034 and No. 52002049). J.M.B. acknowledges support from Welch Foundation (E-1728). X. T. acknowledges support from Sichuan Science and Technology Program (No. 2021YFH0054).

Declaration of Competing Interest

The authors declare that they have no known competing financial interests or personal relationships that could have appeared to influence the work reported in this paper.

Data availability

The original data in this work is available from the corresponding authors upon reasonable requests.

Appendix A. Supplementary data

Supplementary data to this article can be found online at https://doi.org/10.1016/j.mattod.2021.10.022.

References

[1] A. Ashkin, J.M. Dziedzic, Phys. Rev. Lett. 30 (4) (1973) 139.
[2] I.I. Komissarova et al., Opt. Commun. 66 (1) (1988) 15.
[3] G.D. Costa, Appl. Opt. 32 (12) (1993) 2143.
[4] G.D. Costa, J. Calatroni, Appl. Opt. 17 (15) (1978) 2381.
[5] G.D. Costa, J. Calatroni, Appl. Opt. 18 (2) (1979) 233.
[6] H. Helmers, W. Witte, Opt. Commun. 49 (1) (1984) 21.
[7] R.T. Mallea et al., IEEE-ASME Trans. Mechatron. 22 (2) (2017) 693.
[8] J.P. Singer et al., Adv. Mater. 25 (42) (2013) 6100.
[9] J.M. Katzenstein et al., ACS Macro Lett. 1 (10) (2012) 1150.
[10] S.H. Jin et al., Nat. Nanotechnol. 8 (5) (2013) 347.
[11] M. Gugliotti et al., Langmuir 18 (25) (2002) 9792.
[12] L.W. Chen et al., AIP Adv. 9 (4) (2019) 045012.
[13] C. Limmaneevichitr, S. Kou, Weld. J. 79 (5) (2000) 126S.
[14] J. Hartikainen et al., Can. J. Phys. 64 (9) (1986) 1341.
[15] A. Kolomenskii, H.A. Schuessler, Phys. Rev. B 52 (1) (1995) 16.
[16] S.B. Liu et al., Int. J. Therm. Sci. 146 (2019) 106075.
[17] S.A. Khairallah et al., Acta Mater. 108 (2016) 36.
[18] D. Baigl, Lab Chip 12 (19) (2012) 3637.
[19] J.A. Lv et al., Nature 537 (7619) (2016) 179.
[20] M. Grunze, Science 283 (5398) (1999) 41.
[21] A.A. Darhuber, S.M. Troian, Annu. Rev. Fluid Mech. 37 (2005) 425.
[22] S.A. Viznyuk et al., Opt. Commun. 85 (2–3) (1991) 254.
[23] J.-P. Delville et al., Optical Deformability of Fluid Interfaces, Nova Science Publishers, New York, 2009.
[24] J.P. Dery et al., Chem. Mater. 20 (20) (2008) 6420.
[25] W. Wang et al., Nature 559 (7712) (2018) 77.
[26] T. Azami et al., J. Cryst. Growth 233 (1–2) (2001) 99.
[27] S. Fauve, C. R. Phys. 18 (9–10) (2017) 531.
[28] M.J. Block, Nature 178 (4534) (1956) 650.
[29] L.D. Landau, E.M. Lifshitz, *Fluid Mechanics*. 2nd ed., Pergamon Press, 1987, p. 244..
[30] S.M. Pimputkar, S. Ostrach, Phys. Fluids 23 (7) (1980) 1281.
[31] D.L. Hitt, M.K. Smith, Phys. Fluids 5 (11) (1993) 2624.
[32] A. Oron, Phys. Fluids 12 (1) (2000) 29.
[33] I. Seric et al., Phys. Fluids 30 (1) (2018) 012109.
[34] A.V. Hershey, Phys. Rev. 56 (2) (1939) 204.
[35] E. Hasegawa, J. Kojima, Bull. JSME 26 (213) (1983) 380.
[36] H.M.J.M. Wedershoven et al., Appl. Phys. Lett. 104 (5) (2014) 054101.
[37] F. Laeri et al., Opt. Commun. 34 (1) (1980) 23.
[38] W. Batson et al., J. Fluid Mech. 872 (2019) 928.
[39] A. Karbalaei et al., Micromachines 7 (1) (2016) 13.
[40] J.J. Chen et al., Adv. Opt. Mater. 8 (1) (2020) 1900829.
[41] R.E. Rosensweig, Ferrohydrodynamics., Courier Corporation (1997).
[42] A. Kotnala et al., Nano Lett. 20 (1) (2020) 768.
[43] Y. Wang et al., Sci. Adv. 3 (9) (2017) e1700555.
[44] C. Gao et al., Adv. Funct. Mater. 28 (35) (2018) 1803072.
[45] Y. Nabetani et al., Langmuir 23 (12) (2007) 6725.
[46] A.M. Cazabat et al., Nature 346 (6287) (1990) 824.